Article

Cadmium Toxicity Is Regulated by Peroxisome Proliferator-Activated Receptor δ in Human Proximal Tubular Cells

Chikage Mori, Jin-Yong Lee, Maki Tokumoto and Masahiko Satoh *

Laboratory of Pharmaceutical Health Sciences, School of Pharmacy, Aichi Gakuin University,
1-100 Kusumoto-cho, Chikusa-ku, Nagoya 464-8650, Japan; ag193a01@dpc.agu.ac.jp (C.M.);
leejy@dpc.agu.ac.jp (J.-Y.L.); maki@dpc.agu.ac.jp (M.T.)
* Correspondence: masahiko@dpc.agu.ac.jp

Abstract: Cadmium (Cd) is a toxic heavy metal that is widely present in the environment. Renal proximal tubule disorder is the main symptom of Cd chronic poisoning. Our previous study demonstrated that Cd inhibits the total activities of peroxisome proliferator-activated receptor (PPAR) transcription factors in human and rat proximal tubular cells. In this study, we investigated the involvement of PPAR in Cd renal toxicity using the HK-2 human proximal tubular cell line. Among PPAR isoform genes, only *PPARD* knockdown significantly showed resistance to Cd toxicity in HK-2 cells. The transcriptional activity of PPARδ was decreased not only by *PPARD* knockdown but also by Cd treatment. DNA microarray analysis showed that *PPARD* knockdown changed the expression of apoptosis-related genes in HK-2 cells. *PPARD* knockdown decreased apoptosis signals and caspase-3 activity induced by Cd treatment. *PPARD* knockdown did not affect the intracellular Cd level after Cd treatment. These results suggest that PPARδ plays a critical role in the modification of susceptibility to Cd renal toxicity and that the apoptosis pathway may be involved in PPARδ-related Cd toxicity.

1. Introduction

Cadmium (Cd) is an environmentally toxic metal that adversely affects various tissues such as kidney, liver, and lung [1,2]. Because Cd has a long biological half-life (15–30 years), it accumulates in the kidney and liver upon chronic exposure through dietary intake of contaminated rice, vegetables, fish, and shellfish [1,2]. Several decades ago, many areas in Japan were affected by Cd contamination caused by mining, and long-term Cd ingestion causes renal toxicity [3]. Moreover, it is well known that *itai-itai* disease was caused by Cd concentration in Toyama, Japan [3]. Proximal tubular cells are the primary target of Cd-induced renal toxicity. Cd causes cell death through necrosis, apoptosis, autophagy, disruption of cell–cell adhesions, and production of reactive oxygen species in various tissues, including mouse kidney, and cultured cells [4–6]. Among the toxic pathways, cell death of proximal tubular cells of the kidney via the apoptotic pathway is one of the major events of Cd-induced nephrotoxicity.

Our recent studies show that changes in transcriptional activity may be involved in Cd renal toxicity [7–9]. Cd decreases the activity of transcription factor MEF2A in HK-2 human proximal tubular cells [9]. MEF2A regulates the expression of GLUT4. Cd decreases the cellular levels of GLUT4 and the transportation of glucose into cells. The decreased glucose level affects ATP production, which causes cytotoxicity in Cd-treated HK-2 cells [9].

Our previous studies demonstrated that Cd inhibits the activities of peroxisome proliferator-activated receptor (PPAR) transcription factors in human and rat proximal tubular cells [8,10]. PPARs belong to the nuclear receptor superfamily of transcription factors and have three isoforms (PPARα, PPARδ, and PPARγ) in humans. PPARs form

heterodimers with the retinoid X receptor (RXR) and bind to specific DNA elements [11–13]. PPAR affects lipid metabolism, regulation of glucose homeostasis, cell proliferation, differentiation, and apoptosis. PPARα is abundant in tissues with active fatty acid conversion, such as the liver, heart, and digestive tract, and has functions such as fatty acid metabolism and anti-inflammatory actions [14]. PPARγ is mainly expressed in adipose tissue and the immune system, which functions in adipocyte differentiation and insulin regulation [14]. PPARδ is present in various tissues, such as the small intestine, colon, liver, and even cancer tissues; moreover, it regulates metabolism, inflammation, and cell proliferation [14–17].

As described above, PPARs play diverse and important physiological roles. Furthermore, we have demonstrated that Cd changed the transcriptional activity of PPAR. However, the roles of PPAR in the Cd renal toxicity has not been elucidated. Therefore, this study investigated the effect of PPAR knockdown on Cd toxicity and the role of PPAR in Cd-induced apoptosis of HK-2 cells.

2. Results

2.1. Identification of PPAR Affecting Cd Toxicity in HK-2 Cells

To investigate the involvement of PPAR in Cd toxicity in HK-2 cells, we examined the effect of knockdown of each *PPAR* gene on Cd toxicity. In human cells, PPARs consist of PPARα (*PPARA*), PPARδ (*PPARD*), and PPARγ (*PPARG*). Among the isoforms, only *PPARD* knockdown significantly conferred resistance to Cd toxicity (Figure 1A,B). Additionally, each siRNA against *PPAR* genes significantly reduced their mRNA levels in HK-2 cells (Figure 1C).
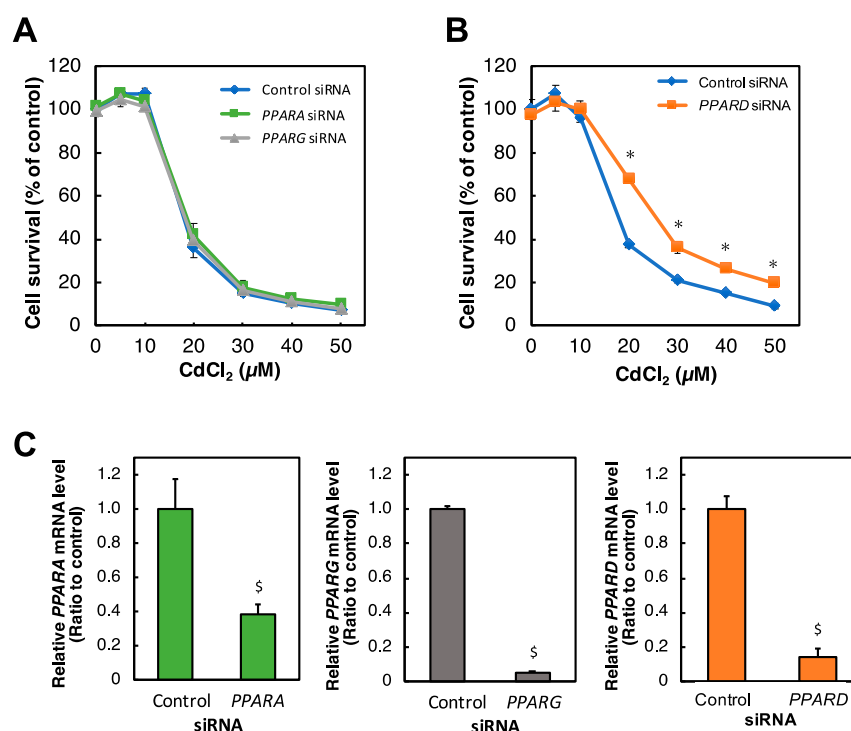
Figure 1. Effect of *PPAR* knockdown on the survival rate of HK-2 cells treated with Cd. (**A**,**B**) After treatment with *PPARA*, *PPARG* or *PPARD* siRNA for 48 h, HK-2 cells were treated with Cd for 24 h. Cell survival was examined by an Alamar blue assay. Values are means ± SD (*n* = 3). * Significantly different from the control siRNA group, *p* < 0.05. (**A**) *PPARA* siRNA and *PPARG* siRNA. (**B**) *PPARD* siRNA. (**C**) Efficiency of *PPARA*, *PPARG*, and *PPARD* knockdown was examined after HK-2 cells were treated with siRNA against the gene of *PPARA*, *PPARG* or *PPARD* for 48 h. *PPARA*, *PPARG*, and *PPARD* mRNA levels were examined by real-time RT-PCR and normalized to *GAPDH* mRNA levels. Values are means ± SD (*n* = 3). $ Significantly different from the control group, *p* < 0.05.

2.2. Effects of Cd and PPARD Knockdown on the PPARδ Transcriptional Activity in HK-2 Cells

To investigate the transcriptional activity of PPARδ by exposure to Cd and *PPARD* knockdown, we examined PPARδ transcriptional activity in Cd-treated or *PPARD* knockdown HK-2 cells. Cd treatment for 6 h significantly and dose-dependently decreased PPARδ transcriptional activity in HK-2 cells (Figure 2A). PPARδ transcriptional activity was significantly decreased after *PPARD* knockdown in HK-2 cells (Figure 2B).
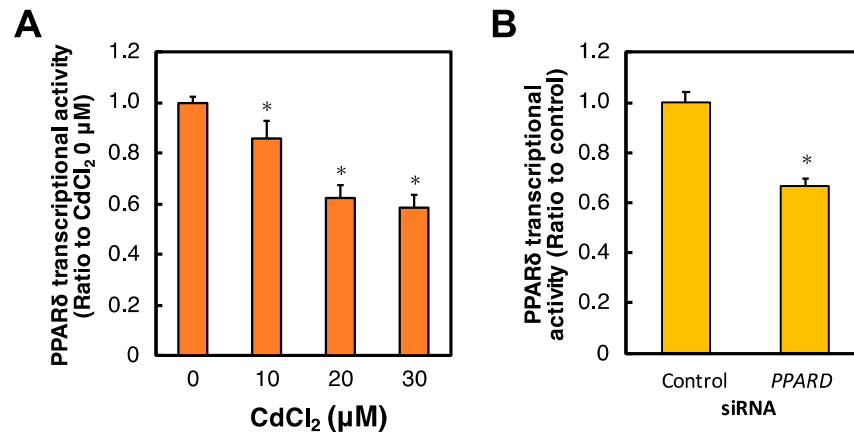
Figure 2. Effect of Cd and *PPARD* knockdown on the PPARδ transcriptional activity in HK-2 cells. (**A**) HK-2 cells were treated with Cd for 6 h. PPARδ transcriptional activity was examined by a PPAR delta Transcriptional Factor Assay Kit after Cd treatment for 6 h. Values are means ± SD (*n* = 3). * Significantly different from the control group, *p* < 0.05. (**B**) PPARδ transcriptional activity by *PPARD* knockdown was examined after HK-2 cells were treated with *PPARD* siRNA for 48 h. Values are means ± SD (*n* = 3). * Significantly different from the control siRNA group, *p* < 0.05.

2.3. Effect of Cd on the PPARD mRNA Level in HK-2 Cells

To clarify the effect of Cd treatment on *PPARD* expression in HK-2 cells, the *PPARD* mRNA level was examined after HK-2 cells were treated with Cd. Cd treatment for 6 h significantly and dose-dependently increased the *PPARD* mRNA level in HK-2 cells (Figure 3). This result implies that the gene expression of *PPARD* may not contribute to the Cd-inhibited transcriptional activity of PPARδ in HK-2 cells.
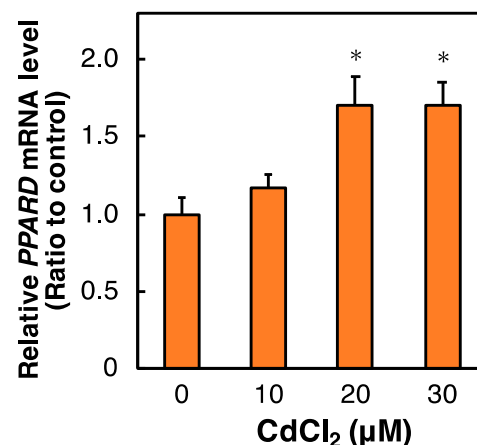
Figure 3. Effect of Cd on the *PPARD* mRNA level in HK-2 cells. HK-2 cells were treated with Cd for 6 h. *PPARD* mRNA levels were examined by real-time RT-PCR after Cd treatment for 6 h. *PPARD* mRNA levels were normalized to *GAPDH* mRNA levels. Values are means ± SD (*n* = 3). * Significantly different from the control group, *p* < 0.05.

2.4. Effect of RXR Knockdown on the Viability of HK-2 Cells Treated with Cd

PPAR forms a dimer with RXR, and therefore resistance to Cd toxicity by *PPARD* knockdown may be associated with RXR activity. To investigate the involvement of RXR in the resistance Cd toxicity by *PPARD* knockdown in HK-2 cells, we examined the effect of *RXR* knockdown on Cd toxicity. RXR also consists of three isoforms [11–13]. Cd cytotoxicity in *RXRA* and *RXRB* knockdown cells was similar to that in control cells (Figure 4A). We also confirmed that *RXRA* and *RXRB* siRNA treatments significantly reduced the levels of *RXRA* and *RXRB* mRNAs in HK-2 cells (Figure 4B). Therefore, RXR may be independent of *PPARD* knockdown-decreased sensitivity to Cd toxicity in HK-2 cells.
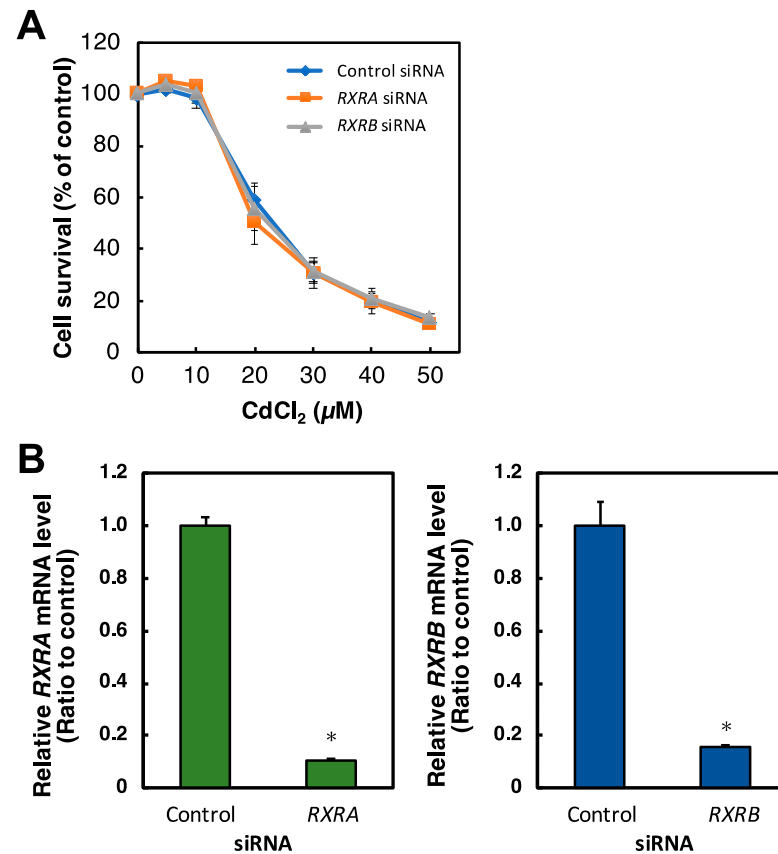
Figure 4. Effect of *RXR* knockdown on the survival rate of HK-2 cells treated with Cd. (**A**) After treatment with siRNA against the gene of *RXRA* or *RXRB* for 48 h, HK-2 cells were treated with Cd for 24 h. Cell survival was examined by the Alamar blue assay. Values are means ± SD (*n* = 3). * Significantly different from the control siRNA group, *p* < 0.05. (**B**) Efficiency of *RXRA* and *RXRB* knockdown was examined after HK-2 cells were treated with siRNA the gene of *RXRA* or *RXRB* for 48 h. *RXRA* and *RXRB* mRNA levels were examined by real-time RT–PCR and normalized to *GAPDH* mRNA levels. Values are means ± SD (*n* = 3). * Significantly different from the control group, *p* < 0.05.

2.5. Identification of Genes Regulated by PPARD Knockdown in HK-2 Cells

PPARδ regulates gene expression by transcriptional activity, and therefore PPARδ-related Cd toxicity may affect downstream factor(s) of PPARδ. To identify genes regulated by PPARδ, we performed DNA microarray analysis of HK-2 cells transfected with PPARD siRNA. PPARD knockdown increased the expression of 53 genes by more than three-fold (Table 1). Among the genes, *RYR2*, *ITPK1*, *PALD1*, *ZNF488*, *TFF2*, *IL9R*, *PANX2*, *CPA4*, *CCL19*, *FSIP1*, and *MLXIPL* are involved in apoptosis [18–28]. *PPARD* knockdown decreased the expression of 39 genes by less than or equal to 0.5-fold (Table 2). Among these genes, *LPAR3*, *GAL3ST1*, *PTPN11*, and *RORA* are involved in apoptosis [29–32]. We examined the effect of Cd on the expression of 15 of the above genes (Figure 5, data not

shown). Cd increased the mRNA levels of *CPA4* and *FSIP1* whose expression was induced by *PPARD* knockdown (Figure 5). Increases in cellular levels of CPA4 and FSIP1 negatively act on apoptosis signals [20,23]. These results indicated that apoptosis was associated with resistance to Cd toxicity by *PPARD* knockdown.
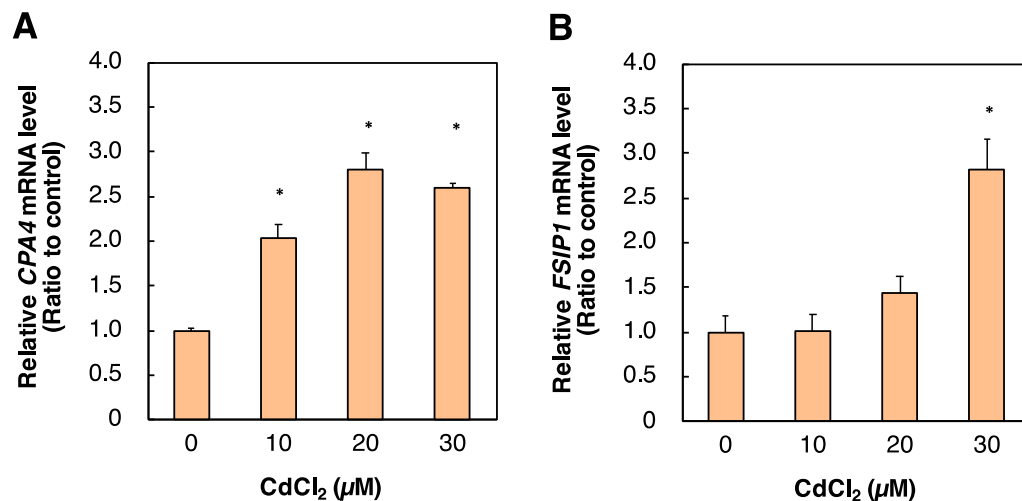
Figure 5. Effect of Cd on *CPA4* and *FSIP1* mRNA levels in HK-2 cells. HK-2 cells were treated with Cd for 6 h. *CPA4* and *FSIP1* mRNA levels were examined by real-time RT–PCR after Cd treatment for 6 h (**A**,**B**). *CPA4* and *FSIP1* mRNA levels were normalized to *GAPDH* mRNA levels. Values are means ± SD ($n = 3$). * Significantly different from the control group, $p < 0.05$.

Table 1. Genes with expression increased by *PPARD* knockdown (>3-fold).

Gene	Accession Number	Description	Fold Change
RYR2	NM_001035	Ryanodine receptor 2	5.75
CDHR2	NM_017675	Cadherin related family member 2	5.31
PCDH19	NM_020766	Protocadherin 19	4.92
TMEM184A	NM_001097620	Transmembrane protein 184A	4.91
GLYAT	NM_005838	Glycine-N-acyltransferase	4.89
AUTS2	NM_001127231	Activator of transcription and developmental regulator AUTS2	4.86
MSR1	NM_002445	Macrophage scavenger receptor 1	4.80
CRLF2	NM_001012288	Cytokine receptor like factor 2	4.77
SLC23A3	NM_144712	Solute carrier family 23 member 3	4.76
IL27	NM_145659	Interleukin 27	4.71
PSG2	NM_031246	Pregnancy specific beta-1-glycoprotein 2	4.70
PITPNM3	NM_031220	PITPNM family member 3	4.46
ITPK1	NM_014216	Inositol-tetrakisphosphate 1-kinase	4.42
ACTN2	NM_001278344	Actinin alpha 2	4.39
BTBD16	NM_001318189	BTB domain containing 16	4.38
PALD1	NM_014431	Phosphatase domain containing paladin 1	4.38
RGS11	NM_003834	Regulator of G protein signaling 11	4.34
SMCO1	NM_001077657	Single-pass membrane protein with coiled-coil domains 1	4.29
ZNF488	NM_153034	Zinc finger protein 488	4.21
GAL3ST1	NM_004861	Pentatricopeptide repeat domain 2	4.20
CACNG7	NM_031896	Calcium voltage-gated channel auxiliary subunit gamma 7	4.19
SERPINF1	NM_002615	Serpin family F member 1	4.19
ESPNL	NM_194312	Espin like	4.19

Table 1. *Cont.*

Gene	Accession Number	Description	Fold Change
LONRF2	NM_198461	LON peptidase N-terminal domain and ring finger 2	4.19
PDE4C	NM_001330172	Phosphodiesterase 4C	4.18
PTPN11	NM_002834	Transmembrane protein 225B	4.16
PRDM11	NM_001359633	PR/SET domain 11	4.11
TFF2	NM_005423	Trefoil factor 2	4.11
PDZD4	NM_032512	PDZ domain containing 4	4.02
CHRNE	NM_000080	Cholinergic receptor nicotinic epsilon subunit	4.01
LRRC3	NM_030891	Leucine rich repeat containing 3	4.00
IL9R	NM_176786	Interleukin 9 receptor	3.94
PANX2	NM_001160300	Pannexin 2	3.88
CPA4	NM_016352	Carboxypeptidase A4	3.76
PLCB1	NM_182734	Phospholipase C beta 1	3.65
TLDC2	NM_080628	TBC/LysM-associated domain containing 2	3.63
PPCDC	NM_134260	Phosphopantothenoylcysteine decarboxylase	3.61
RGMB	NM_001366509	Repulsive guidance molecule BMP co-receptor b	3.51
PDE4DIP	NM_001350522	Phosphodiesterase 4D interacting protein	3.51
RNF125	NM_017831	Ring finger protein 125	3.50
JRK	NM_001279352	Jrk helix-turn-helix protein	3.50
TPRX1	NM_198479	Tetrapeptide repeat homeobox 1	3.44
HAAO	NM_012205	3-Hydroxyanthranilate 3,4-dioxygenase	3.41
SLC43A1	NM_003627	Solute carrier family 43 member 1	3.35
CCL19	NM_006274	C-C motif chemokine ligand 19	3.29
RBM20	NM_001134363	RNA binding motif protein 20	3.23
FSIP1	NM_152597	Fibrous sheath interacting protein 1	3.19
MPZL3	NM_198275	Myelin protein zero like 3	3.18
SMKR1	NM_001195243	Small lysine rich protein 1	3.12
MLXIPL	NM_032951	MLX interacting protein like	3.11
PLXNC1	NM_005761	Plexin C1	3.11
OR6T1	NM_001005187	Olfactory receptor family 6 subfamily T member 1	3.10
EGF	NM_001178130	Epidermal growth factor	3.06

Table 2. Genes with expression decreased by *PPARD* knockdown (≤0.5-fold).

Gene	Accession Number	Description	Fold Change
TTLL9	NM_001035	Tubulin tyrosine ligase like 9	0.10
TNF	NM_000594	Tumor necrosis factor	0.23
SAA1	NM_000331	Serum amyloid A1	0.24
CCL20	NM_004591	C-C motif chemokine ligand 20	0.25
FLG	NM_002016	Filaggrin	0.26
PPARD	NM_006238	Peroxisome proliferator activated receptor delta	0.32
LPAR3	NM_012152	Lysophosphatidic acid receptor 3	0.35
PCOTH	NM_001348114	Pro-X-Gly collagen triple helix like repeat containing	0.36
HACD3	NM_016395	3-Hydroxyacyl-CoA dehydratase 3	0.38
ANKS1B	NM_001352196	Ankyrin repeat and sterile alpha motif domain containing 1B	0.39
TRAK2	NM_015049	Trafficking kinesin protein 2	0.40
ST3GAL6	NM_006100	ST3 beta-galactoside alpha-2,3-sialyltransferase 6	0.40
LTB	NM_014216	Lymphotoxin beta	0.40
UHMK1	NM_175866	U2AF homology motif kinase 1	0.40
DDR1	NM_001202522	Discoidin domain receptor tyrosine kinase 1	0.41

Table 2. *Cont.*

Gene	Accession Number	Description	Fold Change
KCNS3	NM_014431	Potassium voltage-gated channel modifier subfamily S member 3	0.42
SAA2	NM_030754	Serum amyloid A2	0.42
FSIP1	NM_152597	Fibrous sheath interacting protein 1	0.43
EFHC1	NM_153034	EF-hand domain containing 1	0.43
GAL3ST1	NM_004861	Galactose-3-O-sulfotransferase 1	0.43
IL18R1	NM_003855	Interleukin 18 receptor 1	0.44
SGCB	NM_000232	Sarcoglycan beta	0.44
PCDH20	NM_022843	Protocadherin 20	0.44
CA9	NM_001216	Carbonic anhydrase 9	0.44
ZDHHC11B	NM_001351303	Zinc finger DHHC-type containing 11B	0.44
PTPN11	NM_002834	Protein tyrosine phosphatase non-receptor type 11	0.45
CXADR	NM_001338	CXADR Ig-like cell adhesion molecule	0.46
YES1	NM_005423	YES proto-oncogene 1, Src family tyrosine kinase	0.46
LOC391322	NM_032512	D-dopachrome tautomerase-like	0.47
CCDC146	NM_020879	Coiled-coil domain containing 146	0.47
EIF1AY	NM_004681	Eukaryotic translation initiation factor 1A Y-linked	0.47
PTX3	NM_176786	Pentraxin 3	0.47
PTGFRN	NM_001160300	Prostaglandin F2 receptor inhibitor	0.47
CSF2	NM_016352	Colony stimulating factor 2	0.48
ANKRD37	NM_181726	Ankyrin repeat domain 37	0.48
ENTPD2	NM_001246	Ectonucleoside triphosphate diphosphohydrolase 2	0.49
RORA	NM_134260	RAR related orphan receptor A	0.49
PACC1	NM_018252	Proton activated chloride channel 1	0.50
CD83	NM_004233	CD83 molecule	0.50

2.6. Involvement of PPARD Knockdown in Cd-Induced Apoptosis

Previous studies have demonstrated that Cd induces apoptosis in HK-2 cells [4,7,8,33]. Furthermore, some downstream factors of PPARδ are involved in the apoptosis pathway [34,35]. Therefore, we examined whether the resistance to Cd toxicity by *PPARD* knockdown was involved in apoptosis. To compare apoptosis levels, staurosporine (STS) was used as an apoptosis inducer. The apoptosis was significantly induced in control cells by 20 and 30 μM Cd treatment for 12 h. Additionally, Cd-induced apoptosis was significantly inhibited by *PPARD* knockdown. The apoptosis induced by 20 and 30 μM Cd treatment was similar to that induced by 0.1 μM STS treatment for 12 h (Figure 6A). Induction of apoptosis by Cd is mediated through caspase-3 activation in Cd renal toxicity [4]. Therefore, we investigated whether inhibition of Cd-induced apoptosis by *PPARD* knockdown was involved in caspase-3 activation. Cd treatment (10–30 μM) for 9 h increased the level of cleaved caspase-3, whereas *PPARD* knockdown decreased cleaved caspase-3 increased by Cd (Figure 6B). The treatment with 10 μM Cd for 12 h markedly increased the level of cleaved caspase-3 and *PPARD* knockdown decreased the increased one by Cd treatment (Figure 6C). However, the increased level of cleaved caspase-3 by 20 and 30 μM Cd for 12 h was not affected by *PPARD* knockdown. These results indicated that *PPARD* knockdown partly protected HK-2 cells from the Cd-induced apoptosis through a decrease in the cleaved caspase-3 level.
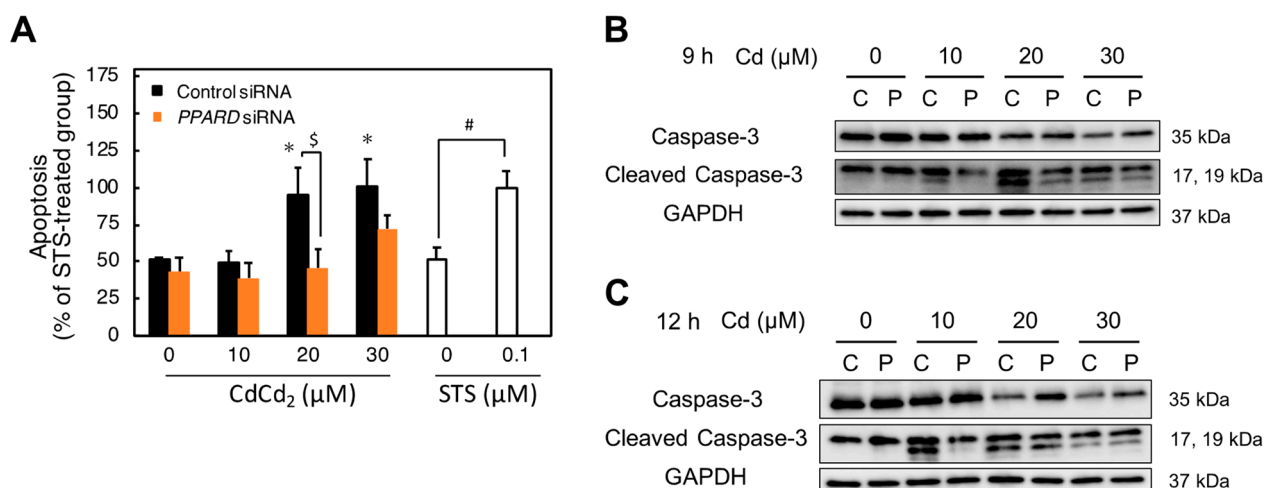
Figure 6. Effect of *PPARD* knockdown on apoptosis of HK-2 cells treated with Cd. (**A**) After treatment with *PPARD* siRNA for 48 h, HK-2 cells were treated with Cd for 12 h. HK-2 cells were treated with STS, as an apoptosis inducer, for 12 h. Apoptosis was examined by a Cell Death Detection ELIZA^{PLUS} Kit after Cd and STS treatment for 12 h. Values are means $\pm$ SD (*n* = 3). * Significantly different from the control siRNA + Cd 0 µM group, $p < 0.05$. $^{\$}$ Significantly different from the control siRNA group, $p < 0.05$. $^{\#}$ Significantly different from the STS 0 µM group, $p < 0.05$. (**B**,**C**) After treatment with *PPARD* siRNA for 48 h, HK-2 cells were treated with Cd for 9 h (**B**) or 12 h (**C**). Protein levels of caspase-3 and cleaved caspase-3 were examined by western blotting after Cd treatment for 9 or 12 h. GAPDH was used as the loading control.

2.7. Effect of PPARD Knockdown on the Intracellular Cd Concentration

PPARD knockdown may affect the Cd accumulation in HK-2 cells. Therefore, we investigated the effect of *PPARD* knockdown on the intracellular Cd concentration after Cd treatment. The intracellular Cd level was increased dose-dependently on the treatment concentration (Figure 7). However, *PPARD* knockdown did not affect the intracellular Cd level (Figure 7).
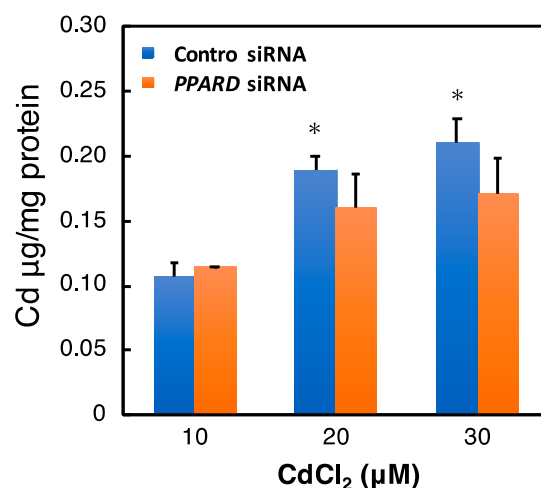
Figure 7. Effect of *PPARD* knockdown on the intracellular Cd concentration. After treatment with *PPARD* siRNA for 48 h, HK-2 cells were treated with Cd for 12 h. The Cd concentration was measured by an atomic absorption spectrometer. Values are means $\pm$ SD (*n* = 3). * Significantly different from the control siRNA + Cd 10 µM group, $p < 0.05$.

3. Discussion

This study strongly suggests that the transcription factor PPARδ modifies susceptibility to Cd toxicity. Additionally, PPARδ transcriptional activity is inhibited in response to Cd stimulation in HK-2 cells. Furthermore, the decrease in PPARδ activity inhibits the apoptosis pathway induced by Cd in HK-2 cells and *PPARD* knockdown is resistant to Cd toxicity in HK-2 cells. The inhibitory effect of Cd on the transcriptional activity of PPARδ may be a biological reaction to protect against Cd toxicity. Moreover, *PPARD* knockdown did not change the concentration of Cd in cells, suggesting that *PPARD* knockdown is not involved in Cd uptake and excretion in HK-2 cells.

Cd increased the level of *PPARD* mRNA. However, transcriptional activity of PPARδ was suppressed by Cd. Therefore, the induction of gene expression of *PPARD* is unlikely to be associated with the suppression of PPARδ transcriptional activity. Several research groups have reported on the regulation of PPARδ activity. In the skeletal muscle, it has been reported that the activity of PPARδ is regulated by AMPK, CRYs, and PGC [36,37]. AMPK promotes PPARδ-dependent transcription. However, AMPK does not increase the PPARδ phosphorylation. AMPK may be present in a transcriptional complex with PPARδ [37]. CRY1 and CRY2 can selectively repress the transcriptional activity of PPARδ [36]. In addition, NCOA6 deficiency suppresses the activity of PPARδ in human and mouse hearts [38,39]. Recent studies demonstrated that Cd changes the AMPK-related pathway and disrupts the expressions of CRY1 [40,41]. These findings suggest that Cd may affect the transcriptional activity of PPARδ via the various mechanisms including the interaction with the cofactors and PPARδ.

Individual differences have been observed in the onset of chronic renal toxicity caused by Cd. Previous studies reported that there are gene polymorphisms in *PPARD* [42,43]. Our study demonstrated that PPARδ is a modification factor in Cd renal toxicity because *PPARD* knockdown is resistant to Cd renal toxicity. The presence of gene polymorphisms in *PPARD* means that there is a population with low PPARδ levels, which may be a population less sensitive to Cd renal toxicity. Moreover, changes in PPARδ may be one of the factors that cause individual differences in the development of Cd renal toxicity. Therefore, these findings suggest PPARδ plays an important role as a modification factor against Cd renal toxicity.

Cd decreases the activities of transcription factors YY1 and FOXF1. As a result, gene expression of the UBE2D family—downstream factors of YY1 and FOXF1—decreases in HK-2 cells [7]. Suppression of UBE2D family expression causes accumulation of apoptosis-inducing factor p53 in the cells, which induces apoptosis [7,33]. Cd decreases transcriptional activity of ARNT in HK-2 cells [8]. The cellular level BIRC3, a downstream factor of ARNT, was decreased by Cd treatment. BIRC3 is an inhibitor of apoptosis. Cd-decreased BIRC3 also induces apoptosis in the HK-2 cells [8]. PPARγ is involved in Cd-induced apoptosis and oxidative stress in renal epithelial cells and hepatocytes [44,45]. In the rat heart cells, DHA (docosahexaenoic acid), which acts as a ligand for PPARδ, has been reported to promote apoptotic cell death, increase caspase-3 activity, and reduce Akt phosphorylation via PPARδ [46]. Furthermore, it has been reported that intracellular prostacyclin promotes apoptosis by activating PPARδ in the human kidney cells [47]. On the other hand, it has also been reported that in mouse brain, PPARδ activation suppresses caspase-3 activation through miR-15a and its downstream Bcl-2 and protects cerebrovascular vessels by reducing apoptosis [48]. We demonstrated that PPARδ is a crucial factor that influences Cd-induced apoptosis in human proximal tubular cells. These findings indicate that Cd triggers renal toxicity via an apoptosis pathway with associations between various related factors. Depending on the various physiological circumstances, there may be differences in the contribution of each apoptosis-related factor to Cd-induced renal toxicity.

4. Materials and Methods

4.1. Cell Culture and Treatment

HK-2 cells purchased from the American Type Culture Collection (Manassas, MA, USA) were cultured in Dulbecco's modified Eagle's medium/Ham's F-12 nutrient mixture (Sigma-Aldrich, St. Louis, MO, USA) containing 10% fetal bovine serum (Gibco, Grand Island, NY, USA), 25 U/mL penicillin (DS Pharm, Osaka, Japan), 25 μg/mL streptomycin (DS Pharm), 1% insulin-transferrin-selenium X (Gibco), 10 ng/mL epidermal growth factor (Sigma-Aldrich), and 5 ng/mL hydrocortisone at 37 °C in a humidified incubator with 5% CO_2. The cells were cultured in test plates at a density of 250 cells/mm^2 for 48 h. After discarding the culture medium, the cells were treated with Cd ($CdCl_2$; 98.0%; Fujifilm Wako Pure Chemical Co., Tokyo, Japan) in serum-free culture medium.

4.2. Small Interfering RNA (siRNA) Transfection

Silencer Select Predesigned siRNAs against human *PPAR* and *RXR* mRNAs were purchased from Ambion (Grand Island, NY, USA). Control siRNA (Silencer Select Negative Control #1 siRNA) was also purchased from Ambion. siRNA transfection was performed with Lipofectamine RNAiMAX (Invitrogen, Grand Island, NY, USA). After the siRNA mixture was incubated for 15 min with Lipofectamine RNAiMAX and Opti-MEM I Reduced Serum Medium (Opti-MEM; Gibco), HK-2 cells were transfected with the siRNA mixture (1 nM siRNA per sequence, 0.2% Lipofectamine RNAiMAX, and 10% Opti-MEM) for 48 h.

4.3. Cell Survival Rate

HK-2 cells were treated with the siRNA mixture in 96-well plates for 48 h. After treatment, Alamar blue (10%; Invitrogen) was added and the cells were incubated for 4 h at 37 °C. Fluorescence was measured at an excitation wavelength of 540 nm and emission wavelength of 595 nm with a SpectraMax® iD3 microplate reader (Molecular Devices, San Jose, CA, USA).

4.4. RNA Extraction

HK-2 cells were treated with the siRNA mixture and Cd in 6-well plates. Cd-treated HK-2 cells were washed twice with ice-cold phosphate-buffered saline (PBS(−); Nissui, Tokyo, Japan). Total RNA was extracted with a PureLink™ RNA Mini Kit (Ambion) in accordance with the manufacturer's instructions. RNA quantity and purity were measured using a BioSpec-nano spectrophotometer (Shimadzu, Kyoto, Japan).

4.5. DNA Microarray Analysis

DNA microarray analysis was performed by Hokkaido System Science Co., Ltd. (Sapporo, Japan). Complementary RNA (cRNA) was synthesized from 50 ng total RNA using a Low Input Quick Amp Labeling Kit (Agilent Technologies, Santa Clara, CA, USA). HK-2 cells were treated with the siRNA mixture in 6-well plates for 48 h. The total RNAs were pooled from the independent three samples. Double-stranded cDNA from control siRNA- or *PPARD* siRNA-treated cells was transcribed in the presence of cyanine (Cy) 3-CTP or Cy5-CTP, respectively. These two sets of labeled cRNAs (300 ng each) were mixed and hybridized to a SurePrint G3 Human 8 × 60 K ver. 3.0 (Agilent Technologies) by a Gene Expression Hybridization Kit (Agilent Technologies) for 17 h at 65 °C. Fluorescent images were recorded with the Agilent Microarray Scanner (G2600D). Digitized image data were processed with Agilent Feature Extraction ver. 12.0.3.1. Information on each gene was obtained from the National Center for Biotechnology Information database.

4.6. Real-Time Reverse Transcription (RT)-PCR

To generate cDNA, total RNA was subjected to a PrimeScript RT Reagent Kit (Perfect Real Time) (Takara Bio, Shiga, Japan). Real-time PCR was performed with SYBR® Premix Ex Taq™ II (Perfect Real Time) (Takara Bio) on the Thermal Cycler Dice Real Time System (Takara Bio). The thermal cycling conditions were 10 s at 95 °C followed by

40 cycles of 5 s at 95 °C and 30 s at 60 °C. Gene expression was normalized to *GAPDH* mRNA levels. The oligonucleotide sequences of the primers used were as follows: sense, 5′-GAAACAGGCCTTCTCAGTGC-3′ and antisense, 5′-TTGCTGGGTCGTCTTTTTCT-3′ for the human *PPARD* gene; sense, 5′-ACGATTCGACTCAAGCTGGT-3′ and antisense, 5′-GTTGTGTGACATCCCGACAG-3′ for the human *PPARA* gene; sense, 5′-TTCAGAAATGCC TTGCAGTG-3′ and antisense, 5′-CCAACAGCTTCTCCTTCTCG-3′ for the human *PPARG* gene; sense, 5′-CAAGGACTGCCTGATTGACA-3′ and antisense, 5′-CTGGTCGACTCCAC CTCATT-3′ for the human *RXRA* gene; sense, 5′-CCTGAGGGCAATCATTCTGT-3′, and antisense, 5′-CCTGCTGCTCAGGGTACTTC-3′ for the human *RXRB* gene; sense, 5′-GCACCG TCAAGGCTGAGAAC-3′ and antisense, 5′-TGGTGAAGACGCCAGTGGA-3′ for the human *GAPDH* gene.

4.7. Western Blot Analysis

HK-2 cells were treated with the siRNA mixture and Cd in 6 cm dishes. After treatment, the cells were washed twice with ice-cold PBS(−) and harvested in RIPA buffer (25 mM Tris, pH 7.6, 150 mM NaCl, 1% NP-40, 1% sodium deoxycholate, and 0.1% sodium dodecyl sulfate (SDS); Thermo Fisher Scientific, Waltham, MA, USA). Protein concentrations were measured by Pierce^{TM} BCA Protein Assay Kit (Thermo Fisher Scientific). Protein samples were separated on an SDS-polyacrylamide gel and transferred to a polyvinylidene difluoride membrane. The membrane was probed with primary antibodies and then with a horseradish peroxidase-conjugated secondary antibody (1:10,000 dilution; GE Healthcare, Little Chalfont, UK). The proteins were detected by enhanced chemiluminescence using Chemi-Lumi One Super (Nacalai Tesque, Kyoto, Japan). Chemiluminescence images were acquired with the ChemiDoc^{TM} imaging system (BIO-RAD, Hercules, CA, USA). The primary antibodies were anti-GAPDH (1:1000 dilution) from American Research Products (Waltham, MA, USA), and anti-Caspase-3 (1:1000 dilution) and anti-Cleaved Caspase-3 (diluted 1:1000) from Cell Signaling Technology (Danvers, MA, USA).

4.8. Nuclear Protein Extraction

Nuclei were extracted with a Nuclear Extraction Kit (ab113474; abcam, Tokyo, Japan). HK-2 cells were treated with Cd or the siRNA mixture in 10 cm dishes. The treated cells were pooled from the independent two samples. After treatment, HK-2 cells were washed twice with ice-cold PBS(−) and harvested in PBS(−). The cells were shaken at $200\times g$ for 10 min at 4 °C in Pre-extraction Buffer that included a Protease Inhibitor Cocktail and dithiothreitol (DTT). The cytoplasmic fraction was collected by centrifugation at $14,000\times g$ for 3 min at 4 °C. The nuclear pellet was resuspended in Extraction Buffer, which included the Protease Inhibitor Cocktail and DTT, and incubated at 4 °C for 1 h with agitation every 15 min. The mixture was centrifuged at $16,000\times g$ for 10 min at 4 °C, and the supernatant was collected. Protein concentrations were measured by Pierce^{TM} BCA Protein Assay Kit.

4.9. PPARδ Transcriptional Activity Assay

PPARδ transcriptional activity was determined by a PPAR delta Transcriptional Factor Assay Kit (ab133106; abcam). After treatment, nuclei were extracted from HK-2 cells. Complete Transcription Factor Binding Assay Buffer (CTFB) was prepared by adding Transcription Factor Binding Assay Buffer, Reagent A, and DTT. Nuclei and CTFB were added to 96-well plates. After covering the 96-well plates with the included cover, the plates were incubated overnight at 4 °C without agitation. The 96-well plates were washed five times with Wash Buffer. Transcription Factor PPAR delta Primary Antibody was prepared by adding Transcription Factor Antibody Binding Buffer (ABB) and PPAR delta Primary Antibody. After completely removing the Wash Buffer, Transcription Factor PPAR delta Primary Antibody was added to the 96-well plates. After covering the 96-well plates with the included cover, the plates were incubated for 1 h at room temperature without agitation. The 96-well plates were then washed five times with Wash Buffer. Transcription Factor Goat Anti-Rabbit HRP conjugate was prepared by adding ABB and Goat Anti-Rabbit

HRP conjugate. After completely removing the Wash Buffer, Transcription Factor Goat Anti-Rabbit HRP conjugate was added to the 96-well plates. After covering the 96-well plates with the included cover, the plates were incubated for 1 h at room temperature without agitation. The 96-well plates were washed five times with Wash Buffer. After completely removing the Wash Buffer, Transcription Factor Developing Solution was added to the 96-well plates. The 96-well plates were incubated for 45 min at room temperature with gentle agitation while protected from light. Absorbance at 450 nm was read within 5 min after adding Stop Solution to the 96-well plate with an iMark[TM] Microplate Reader (BIO-RAD).

4.10. Apoptosis Assay

Apoptosis was examined by a Cell Death Detection ELIZA[PLUS] Kit (Roche, Basel, Switzerland). HK-2 cells were treated with the siRNA mixture and Cd in 96-well plates. After treatment, the HK-2 cells were washed twice with ice-cold PBS(−). Lysis Buffer was added to the cells, followed by incubation for 30 min at room temperature to lyse the cells. The cell lysates were repeatedly pipetted and then transferred to 96-well plates. Incubation buffer containing Anti-Histone Biotin and Anti-DNA POD was added to the 96-well plates. After covering with a close contact cover, the mixture was incubated at room temperature for 2 h while shaking at 300 rpm. The 96-well plate was washed three times with Incubation Buffer and then the Incubation Buffer was completely removed. ABTS solution, in which ABTS tablets were dissolved in the Substrate Buffer, was placed in a 96-well plate and incubated for 20 min with shaking at 250 rpm. After adding the ABTS stop solution, the absorbance was measured at 405 nm and 490 nm with the SpectraMax® iD3 microplate reader. Staurosporine (STS) was used for the positive control treatment [49]. The degree of Cd-induced apoptosis was normalized to apoptosis induced by 0.1 µM STS treatment (12 h).

4.11. Determination of Cd Content

After siRNA or Cd treatment using 6-well plates, cells were washed twice with ice-cold PBS(−) and then three times with PBS(−) containing 2 nM ethylene glycol tetraacetic acid (Nacalai Tesque). The cells were then harvested in 1 mL RIPA buffer and digested with nitric acid and hydrogen peroxide. After sample digestion, metal analysis was carried out using an atomic absorption spectrometer (200 series AA; Agilent Technologies). Protein concentrations were measured by Pierce[TM] BCA Protein Assay Kit to normalize the Cd content.

4.12. Statistical Analysis

Statistical analyses were performed by one- or two-way ANOVA. When the *F*-value was significant ($p < 0.05$), Bonferroni's multiple *t*-test was performed for *post-hoc* comparison ($p < 0.05$). Statistical analyses were performed with SPSS Statistics (IBM, Tokyo, Japan).

Author Contributions: C.M.: experiments and writing—original draft preparation; J.-Y.L.: design of experiments, analyses, and writing—review and editing; M.T.: analyses; M.S.: supervision, funding acquisition, and writing—review and editing. All authors have read and agreed to the published version of the manuscript.

Informed Consent Statement: Not applicable.

Conflicts of Interest: The authors declare no conflict of interest.

References

1. Åkesson, A.; Barregard, L.; Bergdahl, I.A.; Nordberg, G.F.; Nordberg, M.; Skerfving, S. Non-Renal Effects and the Risk Assessment of Environmental Cadmium Exposure. *Environ. Health Perspect.* **2014**, *122*, 431–438. [CrossRef] [PubMed]
2. Järup, L.; Åkesson, A. Current status of cadmium as an environmental health problem. *Toxicol. Appl. Pharmacol.* **2009**, *238*, 201–208. [CrossRef] [PubMed]
3. Aoshima, K. Itai-itai disease: Lessons from the investigations of environmental epidemiology conducted in the 1970's, with special reference to the studies of the Toyama Institute of Health. *Nihon Eiseigaku Zasshi* **2017**, *72*, 149–158. [CrossRef] [PubMed]
4. Fujiwara, Y.; Lee, J.-Y.; Tokumoto, M.; Satoh, M. Cadmium Renal Toxicity via Apoptotic Pathways. *Biol. Pharm. Bull.* **2012**, *35*, 1892–1897. [CrossRef] [PubMed]
5. Lee, J.-Y.; Tokumoto, M.; Satoh, M. Novel Mechanisms of Cadmium-Induced Toxicity in Renal Cells. In *Cadmium Toxicity: New Aspects in Human Disease, Rice Contamination, and Cytotoxicity*; Himeno, S., Aoshima, K., Eds.; Springer: Singapore, 2019; pp. 153–162.
6. Tokumoto, M.; Lee, J.-Y.; Satoh, M. Transcription Factors and Downstream Genes in Cadmium Toxicity. *Biol. Pharm. Bull.* **2019**, *42*, 1083–1088. [CrossRef]
7. Lee, J.-Y.; Tokumoto, M.; Fujiwara, Y.; Hasegawa, T.; Seko, Y.; Shimada, A.; Satoh, M. Accumulation of p53 via down-regulation of UBE2D family genes is a critical pathway for cadmium-induced renal toxicity. *Sci. Rep.* **2016**, *6*, 21968. [CrossRef]
8. Lee, J.-Y.; Tokumoto, M.; Hwang, G.-W.; Lee, M.-Y.; Satoh, M. Identification of ARNT-regulated BIRC3 as the target factor in cadmium renal toxicity. *Sci. Rep.* **2017**, *7*, 17287. [CrossRef]
9. Lee, J.; Tokumoto, M.; Satoh, M. Cadmium toxicity mediated by the inhibition of SLC2A4 expression in human proximal Tubule cells. *FASEB J.* **2020**, *35*, e21236. [CrossRef]
10. Tokumoto, M.; Lee, J.-Y.; Fujiwara, Y.; Satoh, M. Alteration of DNA binding activity of transcription factors in NRK-52E rat proximal tubular cells treated with cadmium. *J. Toxicol. Sci.* **2014**, *39*, 735–738. [CrossRef]
11. Burns, K.A.; Heuvel, J.P.V. Modulation of PPAR activity via phosphorylation. *Biochim. Biophys. Acta (BBA) Mol. Cell Biol. Lipids* **2007**, *1771*, 952–960. [CrossRef] [PubMed]
12. Desvergne, B.; Wahli, W. Peroxisome Proliferator-Activated Receptors: Nuclear Control of Metabolism. *Endocr. Rev.* **1999**, *20*, 649–688. [CrossRef]
13. Juge-Aubry, C.; Pernin, A.; Favez, T.; Burger, A.G.; Wahli, W.; Meier, C.A.; Desvergne, B. DNA Binding Properties of Peroxisome Proliferator-activated Receptor Subtypes on Various Natural Peroxisome Proliferator Response Elements. Importance of the 5′-flanking region. *J. Biol. Chem.* **1997**, *272*, 25252–25259. [CrossRef] [PubMed]
14. Finck, B.N. The PPAR regulatory system in cardiac physiology and disease. *Cardiovasc. Res.* **2007**, *73*, 269–277. [CrossRef]
15. Liu, Y.; Colby, J.K.; Zuo, X.; Jaoude, J.; Wei, D.; Shureiqi, I. The Role of PPAR-δ in Metabolism, Inflammation, and Cancer: Many Characters of a Critical Transcription Factor. *Int. J. Mol. Sci.* **2018**, *19*, 3339. [CrossRef] [PubMed]
16. Peters, J.M.; Gonzalez, F.J. Sorting out the functional role(s) of peroxisome proliferator-activated receptor-beta/delta (PPAR-beta/delta) in cell proliferation and cancer. *Biochim. Biophys. Acta* **2009**, *1796*, 230–241. [PubMed]
17. Wang, Y.X.; Zhang, C.L.; Yu, R.T.; Cho, H.K.; Nelson, M.C.; Bayuga-Ocampo, C.R.; Ham, J.; Kang, H.; Evans, R.M. Regulation of muscle fiber type and running endurance by PPARdelta. *PLoS Biol.* **2004**, *2*, e294. [CrossRef]
18. Berchtold, L.A.; Miani, M.; Diep, T.A.; Madsen, A.N.; Cigliola, V.; Colli, M.; Krivokapic, J.M.; Pociot, F.; Eizirik, D.L.; Meda, P.; et al. Pannexin-2-deficiency sensitizes pancreatic β-cells to cytokine-induced apoptosis in vitro and impairs glucose tolerance in vivo. *Mol. Cell. Endocrinol.* **2017**, *448*, 108–121. [CrossRef] [PubMed]
19. Egaña, I.; Kaito, H.; Nitzsche, A.; Becker, L.; Ballester-Lopez, C.; Niaudet, C.; Petkova, M.; Liu, W.; Vanlandewijck, M.; Vernaleken, A.; et al. Female mice lacking Pald1 exhibit endothelial cell apoptosis and emphysema. *Sci. Rep.* **2017**, *7*, 15453. [CrossRef]
20. Fu, Y.; Su, L.; Cai, M.; Yao, B.; Xiao, S.; He, Q.; Xu, L.; Yang, L.; Zhao, C.; Wan, T.; et al. Downregulation of CPA4 inhibits non small–cell lung cancer growth by suppressing the AKT/c-MYC pathway. *Mol. Carcinog.* **2019**, *58*, 2026–2039. [CrossRef]
21. Johnson, J.D.; Han, Z.; Otani, K.; Ye, H.; Zhang, Y.; Wu, H.; Horikawa, Y.; Misler, S.; Bell, G.I.; Polonsky, K.S. RyR2 and Calpain-10 Delineate a Novel Apoptosis Pathway in Pancreatic Islets. *J. Biol. Chem.* **2004**, *279*, 24794–24802. [CrossRef]
22. Kim, N.; Yu, L.; Dawe, R.; Petyuk, V.A.; Gaiteri, C.; De Jager, P.L.; Schneider, J.A.; Arfanakis, K.; Bennett, D.A. Microstructural changes in the brain mediate the association of AK4, IGFBP5, HSPB2, and ITPK1 with cognitive decline. *Neurobiol. Aging* **2019**, *84*, 17–25. [CrossRef] [PubMed]
23. Liu, T.; Zhang, H.; Sun, L.; Zhao, D.; Liu, P.; Yan, M.; Zaidi, N.; Izadmehr, S.; Gupta, A.; Abu-Amer, W.; et al. FSIP1 binds HER2 directly to regulate breast cancer growth and invasiveness. *Proc. Natl. Acad. Sci. USA* **2017**, *114*, 7683–7688. [CrossRef] [PubMed]
24. Poungvarin, N.; Lee, J.K.; Yechoor, V.K.; Li, M.V.; Assavapokee, T.; Suksaranjit, P.; Thepsongwajja, J.J.; Saha, P.K.; Oka, K.; Chan, L. Carbohydrate response element-binding protein (ChREBP) plays a pivotal role in beta cell glucotoxicity. *Diabetologia* **2012**, *55*, 1783–1796. [CrossRef] [PubMed]
25. Shang, Y.; Kakinuma, S.; Nishimura, M.; Kobayashi, Y.; Nagata, K.; Shimada, Y. Interleukin-9 receptor gene is transcriptionally regulated by nucleolin in T-Cell lymphoma cells. *Mol. Carcinog.* **2011**, *51*, 619–627. [CrossRef] [PubMed]
26. Tu, S.P.; Chi, A.L.; Ai, W.; Takaishi, S.; Dubeykovskaya, Z.; Quante, M.; Fox, J.G.; Wang, T.C. p53 inhibition of AP1-dependent TFF2 expression induces apoptosis and inhibits cell migration in gastric cancer cells. *Am. J. Physiol. Liver Physiol.* **2009**, *297*, G385–G396. [CrossRef]

27. Zhang, X.; Wang, Y.; Cao, Y.; Zhang, X.; Zhao, H. Increased CCL19 expression is associated with progression in cervical cancer. *Oncotarget* **2017**, *8*, 73817–73825. [CrossRef] [PubMed]

28. Zong, D.; Jiang, N.; Xu, J.-H.; Wang, D.-J.; Zhu, H.-F.; Wu, L.-R.; Chen, C.; Yin, L.; He, X. ZNF488 is an independent prognostic indicator in nasopharyngeal carcinoma and promotes cell adhesion and proliferation via collagen IV/FAK/AKT/Cyclin D1 pathway. *Cancer Manag. Res.* **2019**, *ume 11*, 5871–5882. [CrossRef]

29. Chitranshi, N.; Dheer, Y.; Gupta, V.; Abbasi, M.; Mirzaei, M.; You, Y.; Chung, R.; Graham, S.L.; Gupta, V. PTPN11 induces endoplasmic stress and apoptosis in SH-SY5Y cells. *Neuroscience* **2017**, *364*, 175–189. [CrossRef]

30. Ding, K.; Yu, Z.H.; Yu, C.; Jia, Y.Y.; He, L.; Liao, C.S.; Li, J.; Zhang, C.J.; Li, Y.J.; Wu, T.C.; et al. Effect of gga-miR-155 on cell proliferation, apoptosis and invasion of Marek's disease virus (MDV) transformed cell line MSB1 by targeting RORA. *BMC Vet. Res.* **2020**, *16*, 23. [CrossRef] [PubMed]

31. Geraldo, L.H.M.; de Sampaio Spohr, T.C.L.; do Amaral, R.F.; da Fonseca, A.C.C.; Garcia, C.; de Almeida Mendes, F.; Freitas, C.; Fabio dosSantos, M.; Lima, F.R.S. Role of lysophosphatidic acid and its receptors in health and disease: Novel therapeutic strategies. *Signal Transduct. Target. Ther.* **2021**, *6*, 45. [CrossRef]

32. Suchanski, J.; Grzegrzolka, J.; Owczarek, T.; Pasikowski, P.; Piotrowska, A.; Kocbach, B.; Nowak, A.; Dziegiel, P.; Wojnar, A.; Ugorski, M. Sulfatide decreases the resistance to stress-induced apoptosis and increases P-selectin-mediated adhesion: A two-edged sword in breast cancer progression. *Breast Cancer Res.* **2018**, *20*, 133. [CrossRef] [PubMed]

33. Tokumoto, M.; Fujiwara, Y.; Shimada, A.; Hasegawa, T.; Seko, Y.; Nagase, H.; Satoh, M. Cadmium toxicity is caused by accumulation of p53 through the down-regulation of Ube2d family genes in vitro and in vivo. *J. Toxicol. Sci.* **2011**, *36*, 191–200. [CrossRef] [PubMed]

34. Hwang, J.S.; Eun, S.Y.; Ham, S.A.; Yoo, T.; Lee, W.J.; Paek, K.S.; Do, J.T.; Lim, D.S.; Seo, H.G. PPARδ modulates oxLDL-induced apoptosis of vascular smooth muscle cells through a TGF-β/FAK signaling axis. *Int. J. Biochem. Cell Biol.* **2015**, *62*, 54–61. [CrossRef] [PubMed]

35. Wu, K.K.; Liou, J.Y. Cyclooxygenase inhibitors induce colon cancer cell apoptosis Via PPARdelta –> 14-3-3epsilon pathway. *Methods Mol. Biol.* **2009**, *512*, 295–307. [PubMed]

36. Jordan, S.D.; Kriebs, A.; Vaughan, M.; Duglan, D.; Fan, W.; Henriksson, E.; Huber, A.L.; Papp, S.J.; Nguyen, M.; Afetian, M.; et al. CRY1/2 Selectively Repress PPARδ and Limit Exercise Capacity. *Cell Metab.* **2017**, *26*, 243–255.e6. [CrossRef]

37. Narkar, V.A.; Downes, M.; Yu, R.T.; Embler, E.; Wang, Y.X.; Banayo, E.; Mihaylova, M.M.; Nelson, M.C.; Zou, Y.; Juguilon, H.; et al. AMPK and PPARdelta agonists are exercise mimetics. *Cell* **2008**, *134*, 405–415. [CrossRef]

38. Mahajan, M.A.; Samuels, H.H. Nuclear receptor coactivator/coregulator NCoA6(NRC) is a pleiotropic coregulator involved in transcription, cell survival, growth and development. *Nucl. Recept. Signal.* **2008**, *6*, e002. [CrossRef]

39. Roh, J.-I.; Cheong, C.; Sung, Y.H.; Lee, J.; Oh, J.; Lee, B.S.; Lee, J.-E.; Gho, Y.S.; Kim, D.-K.; Park, C.B.; et al. Perturbation of NCOA6 Leads to Dilated Cardiomyopathy. *Cell Rep.* **2014**, *8*, 991–998. [CrossRef] [PubMed]

40. Arab, H.H.; Gad, A.M.; Reda, E.; Yahia, R.; Eid, A.H. Activation of autophagy by sitagliptin attenuates cadmium-induced testicular impairment in rats: Targeting AMPK/mTOR and Nrf2/HO-1 pathways. *Life Sci.* **2021**, *269*, 119031. [CrossRef] [PubMed]

41. Jiménez-Ortega, V.; Cano-Barquilla, P.; Scacchi, P.A.; Cardinali, D.P.; Esquifino, A.I. Cadmium-Induced Disruption in 24-h Expression of Clock and Redox Enzyme Genes in Rat Medial Basal Hypothalamus: Prevention by Melatonin. *Front. Neurol.* **2011**, *2*, 13. [CrossRef]

42. Bailén, M.; Tabone, M.; Bressa, C.; Lominchar, M.G.M.; Larrosa, M.; González-Soltero, R. Unraveling Gut Microbiota Signatures Associated with PPARD and PARGC1A Genetic Polymorphisms in a Healthy Population. *Genes* **2022**, *13*, 289. [CrossRef] [PubMed]

43. Hishida, A.; Wakai, K.; Naito, M.; Tamura, T.; Kawai, S.; Hamajima, N.; Oze, I.; Imaizumi, T.; Turin, T.C.; Suzuki, S.; et al. Polymorphisms in PPAR Genes (PPARD, PPARG, and PPARGC1A) and the Risk of Chronic Kidney Disease in Japanese: Cross-Sectional Data from the J-MICC Study. *PPAR Res.* **2013**, *2013*, 980471. [CrossRef] [PubMed]

44. Hosohata, K.; Mise, N.; Kayama, F.; Iwanaga, K. Augmentation of cadmium-induced oxidative cytotoxicity by pioglitazone in renal tubular epithelial cells. *Toxicol. Ind. Health* **2019**, *35*, 530–536. [CrossRef]

45. Wang, H.; Wang, A.; Wang, X.; Zeng, X.; Xing, H. AMPK/PPAR-γ/NF-κB axis participates in ROS-mediated apoptosis and autophagy caused by cadmium in pig liver. *Environ. Pollut.* **2022**, *294*, 118659. [CrossRef] [PubMed]

46. Samokhvalov, V.; Zlobine, I.; Jamieson, K.L.; Jurasz, P.; Chen, C.; Lee, K.S.S.; Hammock, B.D.; Seubert, J.M. PPARδ signaling mediates the cytotoxicity of DHA in H9c2 cells. *Toxicol. Lett.* **2014**, *232*, 10–20. [CrossRef] [PubMed]

47. Hatae, T.; Wada, M.; Yokoyama, C.; Shimonishi, M.; Tanabe, T. Prostacyclin-dependent apoptosis mediated by PPAR delta. *J. Biol. Chem.* **2001**, *276*, 46260–46267. [CrossRef] [PubMed]

48. Yin, K.J.; Deng, Z.; Hamblin, M.; Xiang, Y.; Huang, H.; Zhang, J.; Jiang, X.; Wang, Y.; Chen, Y.E. Peroxisome proliferator-activated receptor delta regulation of miR-15a in ischemia-induced cerebral vascular endothelial injury. *J. Neurosci.* **2010**, *30*, 6398–6408. [CrossRef] [PubMed]

49. Bertrand, R.; Solary, E.; O'Connor, P.; Kohn, K.W.; Pommier, Y. Induction of a Common Pathway of Apoptosis by Staurosporine. *Exp. Cell Res.* **1994**, *211*, 314–321. [CrossRef] [PubMed]